Eur. Phys. J. D **20**, 449–457 (2002)
DOI: 10.1140/epjd/e2002-00159-2

THE EUROPEAN PHYSICAL JOURNAL D

Structures of amide-water neutral complexes from dipole-bound anion formation

F. Lecomte, B. Lucas, G. Grégoire, J.P. Schermann, and C. Desfrançois[a]

Laboratoire de Physique des Lasers, Institut Galilée, Université Paris-Nord, 93430 Villetaneuse, France

Received 13 March 2002
Published online 13 September 2002 –

Abstract. Using Rydberg Electron Transfer Spectroscopy, formation of dipole-bound anion complexes of formamide, N-methylformamide, N,N-dimethylformamide and N-methylacetamide with water has been studied. Each neutral complex can exist with several configurations and the lowest energy structures have been identified through comparison between Density Functional Theory calculations of the neutrals and measured electron binding energies of the observed weakly-bound anions.

PACS. 33.15.Ry Ionization potentials, electron affinities, molecular core binding energy – 36.40.Mr Spectroscopy and geometrical structure of clusters – 82.30.Rs Hydrogen bonding, hydrophilic effects

1 Introduction

The interaction between water and biological molecules is of great importance in a wide range of processes occurring in living organisms. The structure of water in the vicinity of proteins can be quite different from that of pure water [1]. A network of hydrogen bonds involving water molecules stabilizes structures within a protein [2,3] or in between proteins and other biological macromolecules [4]. Statistically, the vast majority of water molecules, which are bound to a protein, establish hydrogen bonds as donors to C=0 groups and to a less extent as acceptors to N–H groups of the peptide chain. Hydration of side-chains is apparently less important, except for charged COO^-groups of Asp and Glu. In order to separate between solvent-induced and intrinsic properties, a number of gas-phase studies have been devoted during recent years to hydration of elementary building blocks of proteins. Enthalpy and entropy changes associated with binding of peptides ions to water molecules have been observed in ion-mobility measurements [5]. Hydration sites of side-chains and model peptides have been precisely determined with the help of molecular beam spectroscopy. Most of these studies take advantage of the well-resolved UV spectra of aromatic side-chain model molecules, like phenol (Tyr) and indole (Trp), and use R2PI (Resonantly Enhanced 2 Photons Ionization) [6], IR-UV depletion [7,8] and MATI [9] spectroscopic techniques. Since the same approach cannot hold for aliphatic amides, R2PI and IR-UV studies of hydration have been conducted on aromatic models of the peptide bond such as N-benzylformamide [10] or oxindole [11].

Complexes of water with non-aromatic amides such as the formamide-water dimer have however been investigated by means of pulsed-nozzle Fourier-transform microwave spectroscopy [12] and far-infrared spectroscopy in argon matrices [13]. Microwave and matrix spectroscopy do not have the mass-discrimination ability provided by resonant ionisation. Interpretation of the spectra is then difficult since water can bind to amides as a donor or an acceptor thus leading to a variety of possible complex structures. Moreover, isolated substituted amides can exist in two different, *cis* or *trans*, conformations [14].

In this work, we take advantage of the large dipole moments of formamide and of several of its methylated derivatives – N-methylformamide, N,N-dimethylformamide and N-methylacetamide – in order to determine the structure of neutral aliphatic amide-water complexes. We use Rydberg Electron Transfer (RET) spectroscopy which is a resonant non-perturbative ionisation technique leading to dipole-bound, or multipole-bound, anions possessing almost the same structures as their neutral parent [15–18]. As in other weakly-bound complex studies, interpretation of data requires a comparison between experimentally determined parameters which are characteristic of each complex structure and predictions of these molecular parameters by means of quantum chemistry calculations. In R2PI, MATI or IR-UV studies, the measured parameters are the UV or IR spectroscopic fingerprints of the complexes as compared to those of the bare molecules: shifts of the first excited electronic state, assignment of vibrational low-frequency modes, shifts of

[a] e-mail: desfranc@galilee.univ-paris13.fr

ionisation potentials or shifts of the vibrational stretch frequencies for intramolecular bonds which are engaged in hydrogen bonds. In RET spectroscopy, we measure the anion formation rates in charge-transfer collisions between Rydberg atoms and the polar neutral molecules or complexes, as a function of the exchanged electron principal quantum number. When dipole-bound anions are created, the dependencies of those anion creation rates are characteristic of the excess electron binding energy which is itself strongly dependent upon the electrostatic and thus structural properties of the neutral complexes.

We will here first briefly recall the experimental procedure and how the experimental value of the excess electron binding energy, also called dipole-bound electron affinity $EA_{\rm db}^{\rm exp}$, is deduced from the experimental data, for each observed complex anion. We will then present Density Functional Theory (DFT) calculations of the low-energy equilibrium structures of the investigated neutral complexes. From the corresponding configurations, we will evaluate theoretical values $EA_{\rm db}^{\rm th}$, by means of an electrostatic model of multipole-bound anions. By comparison between $EA_{\rm db}^{\rm exp}$ and $EA_{\rm db}^{\rm th}$, we will identify the structures of the neutral parents corresponding to the observed weakly-bound complex anions.

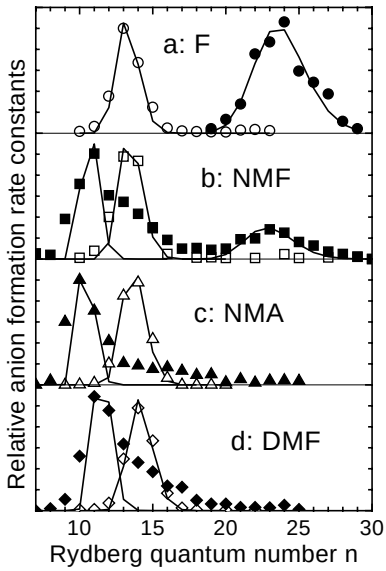

Fig. 1. n-dependencies of the RET anion production rates for formamide (a), N-methylformamide (b), N-methylacetamide (c), N,N-dimethylformamide (d) anions. Open and full points respectively correspond to experimental data for monomers and mono-hydrated complexes. Full curves result from model curve-crossing calculations with fitted anion excess electron binding energies $EA_{\rm db}^{\rm exp}$, as given in Table 1.

2 Experiment

2.1 Set-up

Anions with very weakly bound excess electrons are produced by charge transfer collisions between laser-excited Rydberg atoms and cold neutral polar species. The here used experimental set-up has been described in details in reference [19]. A supersonic neutral molecular cluster beam is created by means of a pulsed valve (General Valve, 0.15 mm conical nozzle) followed by a 2 mm diameter skimmer. For the production of mixed amide-water complexes, we flow few bars of helium over a first reservoir containing water, followed downstream by a second heated reservoir containing formamide or its derivatives. The production of neutral hydrated complexes is optimised by changing the pressure of the helium carrier gas (typically 2 bars), both reservoir temperatures (typically room temperature for the water container and 40–80 °C for the amide container) and the time delay between the opening of the valve and the Rydberg atom creation. In a perpendicular beam, xenon atoms are first excited into metastable states by electron bombardment and further into Rydberg $Xe^{**}(nf)$ states by means of a tunable dye laser (460–500 nm) pumped by a pulsed Nd/YAG laser. Charge-exchange takes place between the beam of laser-excited xenon atoms and the molecular cluster beam in their intersecting region. The created anions are further accelerated and mass-analysed in a time-of-flight tube and they are detected by a set of microchannel plates. The dependencies of the rate constants for anion formation as a function of the principal quantum number n of the xenon Rydberg atoms (n-dependencies) are determined by comparison with SF_6 rate constants due to collisions with a thermal SF_6 beam [20].

2.2 Dipole-bound anion excess electron binding energies

The different n-dependencies of the RET production rates for formamide (F), N-methylformamide (NMF), N,N-dimethylformamide (DMF), and N-methylacetamide (NMA), either isolated or singly hydrated, are displayed in Figure 1. As it can be seen, the charge-exchange process occurs in a limited range of values for the principal quantum number n of the Rydberg atom, in contrast with valence anion production. These peaked n-dependencies of the RET anion production rates are indeed characteristic of the formation of dipole-bound or multipole-bound anions for which the excess electron is weakly bound mainly by the dipole or multipole part of the electron-molecule electrostatic potential. In a first approximation [16,21], experimental values of the excess electron binding energies, $EA_{\rm db}^{\rm exp}$, can be simply deduced from the principal quantum number $n_{\rm max}$ of the Rydberg atoms at which anion formation rates are peaked, with the following empirical law: $EA_{\rm db}^{\rm exp} \approx 23\ {\rm eV}/n_{\rm max}^{2.8}$. In the present work, more accurate values will be obtained by fitting experimental RET curves by means of a curve-crossing model considering the Rydberg atom/polar molecular system charge-transfer process [22]. Full curves in Figures 1a–1d thus correspond to such model calculations in which the only fitting parameter is the anion excess electron binding energy $EA_{\rm db}^{\rm exp}$. The RET curves of isolated F, NMF and DMF

Table 1. Experimental excess electron binding energies $EA_{\rm db}^{\rm exp}$ (meV) for isolated and mono-hydrated complex anions of formamide (F), N-methylformamide (NMF), N-methylacetamide (NMA) and N,N-dimethylformamide (DMF).

amide	F	NMF	NMA	DMF
isolated molecule	16.1	15.4	14.8	13.5
amide-water complex	3.1	3.5		
		29 ± 10	33 ± 10	24 ± 10

Table 2. DFT B3LYP/aug-cc-pVDZ calculation results for isolated monomers. NMF*t* and NMF*c* correspond to eclipsed conformations, NMA*t* and DMF to eclipsed-eclipsed conformations and NMA*c* to staggered-staggered conformation. For F, NMF and DMF, calculated dipole moments are overestimated by 0.2–0.3 D as compared to experimental data. For NMF and NMA *trans* conformers are favoured over *cis* conformers.

monomer	E (a.u.)	$E + ZPE$ (a.u.)	$\mu_{\rm calc}$ (D)	$\mu_{\rm exp}$ (D)	$\Delta(E + ZPE)$ (meV)
water	−76.444643	−76.423414	1.853	1.855	
F	−169.925371	−169.880114	3.975	3.73	
NMF*t*	−209.235197	−209.161465	4.01	3.78–3.83	0
NMF*c*	−209.233478	−209.159890	4.34		43
NMA*t*	−248.560887	−248.459736	3.86	3.70–3.85	0
NMA*c*	−248.557298	−248.456043	4.22		100
DMF	−248.545290	−248.443730	4.16	3.82–3.85	

have already been presented in reference [21] and are here given for the sake of comparison with those of NMA and mixed dimers.

2.3 Results

The monomer anion RET curves are rather similar and exhibit single sharp peaks, for principal Rydberg quantum numbers around 13–14. They are very well fitted by the curve-crossing model calculations and we can accurately deduce the corresponding experimental excess electron binding energies $EA_{\rm db}^{\rm exp}$, as displayed in Table 1. These are slowly decreasing in the order F > NMF > NMA > DMF, as already observed for F, NMF and DMF [21]. As discussed below (see Sect. 4), these values are compatible with the experimental dipole moment values, in the range 3.7–3.9 D (see Tab. 2), even if those are in a different order: NMF (3.78 D [23] or 3.83 D [24]) ≈ DMF (3.82 D [24] or 3.85 D [25]) > F (3.73 D [24]), the experimental dipole moment of NMA being much less well-known (3.7 D [26] to 3.85 D [27]).

The RET curves of the mono-hydrated anion complexes exhibit single peaks at large n-values (around 22–25) for F and at low n-values (around 10–12) for NMA and DMF. Interestingly, the RET curve of the NMF-water anions presents both well-separated peaks, at large and low n-values. Since the four amides possess almost the same dipoles, this strongly suggests that there are at least two possible low-energy configurations for the mono-hydrated complexes: one corresponding to a dipole moment lower than that of monomers, leading to a lower anion excess electron binding energy and to a high-n peak, and one corresponding to a dipole moment higher than that of monomers, leading to a higher anion excess electron binding energy and to a low-n peak. As for monomers, we also fit all peaks in order to deduce the corresponding excess electron binding energies (see Tab. 1). While high-n peaks are again well fitted by the curve-crossing model calculations, we note that low-n peaks are too wide to be as well fitted. The displayed full curves are then the result of a least square fit of the experimental points which belong to the peaks and the obtained $EA_{\rm db}^{\rm exp}$ values correspond to mean values with typical uncertainties of about 10 meV. Qualitatively, these wide low-n peaks indicate either a geometry change between neutral and anion structures, as it has been observed for few other mono-hydrated complexes [28,29], or a superposition of several neutral configurations of similar dipole moments. The full interpretation of these observations will be done in Section 4, with the help of quantum calculations of neutral structures and model calculations of the corresponding dipole-bound anions which we now describe.

3 Calculations

3.1 Quantum calculation method and results for isolated amides

For quantum calculations of neutrals, we choose the Density Functional Theory (DFT) method, together with the Becke's three parameter hybrid functional [30] and the non-local transformed correlation correction functional of Lee-Yang-Par (B3LYP), since it is known to provide fast and accurate results for both monomer conformations and complex configurations [11], especially when valence and hydrogen bonds are mainly involved. All calculations have been performed with the Gaussian98W package [31] and run on AMD Athlon 1.4 GHz PCs. For the basis set, we use the Dunning's aug-cc-pVDZ set which is known to provide accurate electrostatic properties [32]. Concerning dipole moments, as it can be seen from Table 2, this holds

Table 3. DFT B3LYP/aug-cc-pVDZ calculation results for equilibrium configurations of mono-hydrated neutral complexes. All configurations possess no imaginary frequency, *i.e.* they are true minima. For each complex configuration, differences in the total energies ($\Delta(E + ZPE)$) are indicated with respect to the lowest equilibrium configuration with either the same amide conformation or with the lowest amide conformation (in parenthesis for NMF and NMA). Species in bold are the low-lying configurations which are present in the beam and which form dipole-bound anions.

Amide-water complex	E (a.u.)	$E + ZPE$ (a.u.)	$\mu_{\rm calc}$ (D)	$D_{\rm e}$ (meV)	D_0 (meV)	$\Delta(E + ZPE)$ (meV)
F-water A	−246.384164	−246.313715	2.69	385	277	**0**
F-water B	−246.380004	−246.310287	3.94	272	184	93
F-water C	−246.377640	−246.309036	6.46	208	150	127
NMF*t*-water A′	−285.690687	−285.592588	4.02	295	210	**0 (44)**
NMF*t*-water B	−285.690299	−285.592159	4.36	285	198	**12 (56)**
NMF*t*-water C	−285.687001	−285.590294	6.25	195	147	63 (107)
NMF*c*-water A	−285.692832	−285.594218	3.24	400	297	0 (0)
NMF*c*-water B	−285.688741	−285.590595	4.45	289	198	99 (99)
NMA*t*-water B′	−325.017079	−324.891841	4.58	316	236	**0 (0)**
NMA*t*-water A′	−325.016897	−324.891366	4.41	311	223	**13 (13)**
NMA*t*-water C	−325.012496	−324.888342	6.64	191	142	94 (94)
NMA*c*-water A	−325.016914	−324.890797	3.48	407	309	0 (27)
NMA*c*-water B′	−325.013642	−324.887927	4.86	318	230	79 (106)
DMF-water B	−325.000776	−324.874855	4.54	295	210	**0**
DMF-water A′	−325.000538	−324.874616	4.30	289	203	**7**

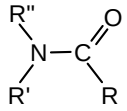

Fig. 2. Sketch of the amide molecules studied in this work. Formamide (F) corresponds to R=R′=R″=H, *trans* N-methylformamide (NMF*t*) to R=R′=H and R″=CH_3, *cis* N-methylformamide (NMF*c*) to R=R″=H and R′=CH_3, *trans* N-methylacetamide (NMA*t*) to R=R″=CH_3 and R′=H, *cis* N-methylacetamide (NMA*c*) to R=R′=CH_3 and R″=H and N,N-dimethylformamide (DMF) to R=H and R′=R″=CH_3.

for water and possibly for NMA but the calculated values for F, NMF and DMF are still about 0.2–0.3 D overestimated as compared to experimental data. Note however that other methods and basis sets do not perform any better for these molecules [21].

The lowest-energy monomer conformations we found are in good agreement with previous studies and Table 2 displays the energetic and dipole moment results. Formamide is strictly planar with C–N and C–O distances equal to 1.362 an 1.218 Å and with a N–C–O angle equal to 124.7° [33]. For N-methylformamide and N-methyl acetamide, there are two, *cis* and *trans*, possible conformations together with two, eclipsed or staggered, conformations for each substituted methyl group (for homogeneity between NMA and NMF, we adopt a convention different from that of references [21,23], as shown in Fig. 2). For NMF, the *trans* conformer (NMF*t*) is found to be more stable than the *cis* one [23] (NMF*c*) by 43 meV, with the methyl group in the eclipsed conformation and a strictly planar heavy atom skeleton, for both conformers. For NMA, the *trans* conformer (NMA*t*) is even more stable (100 meV) as compared to the *cis* one (NMA*c*). The methyl groups are in the eclipsed-eclipsed conformation for NMA*t* and in the staggered-staggered conformation for NMA*c* [27]. The heavy atoms skeleton is still strictly planar for the *trans* conformer but deviates slightly from planarity for the *cis* conformer in which the methyl groups also deviate slightly from the eclipsed position, due to their mutual repulsion. For DMF, the only stable conformation is a true eclipsed-eclipsed one in which all heavy atoms lie again exactly in the same plane. We however note that the potential energy surface corresponding to the methyl group internal rotation is rather flat [23], so that the above equilibrium conformations can easily change upon complexation with one water molecule, as outlined below.

3.2 Equilibrium structures of neutral mono-hydrated complexes

In order to explore as much as possible the configuration space of the mixed amides-water complexes, we first generated initial structures by means of a fast home-made program [29,34,35] which couples an empirical force field, for the intermolecular interactions, to a genetic algorithm, for locating the low-lying minima on the intermolecular potential energy surface. These starting structures were then fully optimised at the B3LYP/aug-cc-pVDZ level, with the default parameters for the convergence criteria, and frequency calculations were then performed. We thus obtained 15 different possible equilibrium structures for the mono-hydrated amide complexes of interest. Their energies and dipole moments are reported in Table 3 and these structures can be rationalised into five configurations, as displayed in Figure 3.

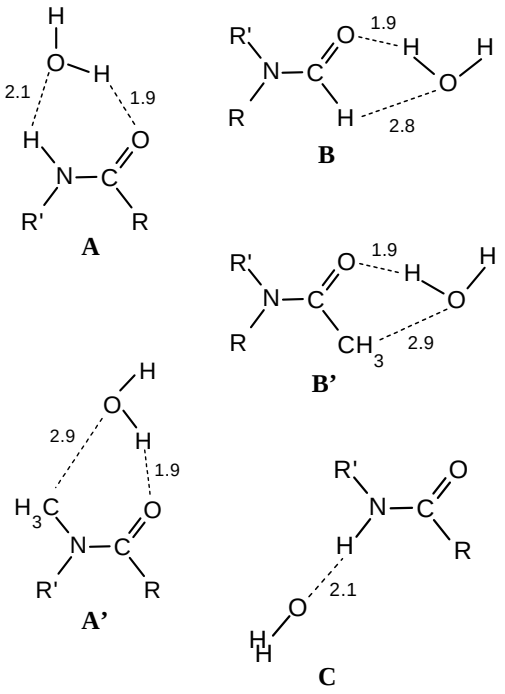

Fig. 3. Sketch of the five types of neutral complex structures for mono-hydrated amide complexes. For A′ and B′ configurations, the oxygen atom of water interacts either with two hydrogen atoms of the amide methyl group (A′ for NMF*t* and A′ and B′ for NMA*t*) or with only one (B′ for NMA*c* and A′ for DMF). Approximate hydrogen bond distances are indicated.

A very stable configuration, further labelled A, involves a double hydrogen bond between the water molecule and the N–H and C=O bonds of the amide molecule, when these two bonds are on the same side of the molecule, *i.e.* for F, NMF*c* and NMA*c*. The D_e and D_0 complex dissociation energies are large, respectively around 400 meV and 300 meV, and the total dipole moment is rather low, in between 2.7 and 3.4 D, because the water and amide dipoles are pointing almost in opposite directions. As far as we know, the only available experimental value for the dipole moment of amide-water complexes is for formamide [12], 2.38 D, which is 0.3 D lower than the present calculated value of 2.69 D. This discrepancy (0.31 D) is almost the same as for the formamide monomer (0.25 D). In agreement with experimental data [36], we note that the true minimum corresponds to a free water OH bond slightly out of the plane of the amide molecule while the planar structure corresponds to a first order saddle point. This stationary point corresponds to a slightly lower dipole moment of 2.43 D and is located only about 1 meV above the maximum. The potential energy surface is thus very flat around this planar structure, along the intermolecular coordinate corresponding to the out-of-plane motion of the free OH bond [13], leading to a very low frequency of about 100 cm^{-1}. This type of structure A is expected to lead to dipole-bound anions with small excess electron binding energies EA_{db}. Another neighbouring configuration, labelled A′, appears when the N–H bond is replaced by a N–CH_3 group on the same side as the C=O bond, *i.e.* for NMF*t*, NMA*t* and DMF. Since the interaction between the water oxygen atom and this N–CH_3 group is now weaker, the dissociation energies are smaller: $D_e \approx 300$ meV and $D_0 \approx 210$ meV. The water dipole is more perpendicular to the amide dipole and the total dipole moment is larger, about 4–4.4 D. These higher values are expected to lead to higher EA_{db} values. In A′ configurations, the water molecule always lies strictly in the same plane as the amide molecule.

In configurations B and B′, the water molecule remains in the plane of the amide molecule and is still hydrogen-bound to the amide C=O bond, but it is now also interacting respectively with either the C–H, for F NMF and DMF, or the C–CH_3 bond, for NMA. Because this second interaction is weaker than a hydrogen bond, B configurations are less stable than A ones: $D_e \approx 280$ meV and $D_0 \approx 200$ meV. On the other hand, a methyl group bound to the amide carbon atom seems to be slightly more electropositive than one bound on the nitrogen atom since B′ configurations are slightly more stable than A′ ones: $D_e \approx 320$ meV, $D_0 \approx 230$ meV. The fact that B′ structures are more stable than B ones is not so surprising because it is well-known that a methyl group is more electropositive than a simple hydrogen atom. The dipole moment orientations are more favourable and the total dipole is about 3.9–4.5 D for B and 4.6–4.9 D for B′, *i.e.* similar to those for A′ configurations. EA_{db} values are thus expected to be similar too.

Finally, a fifth configuration, labelled C, involves a water molecule acting as a proton acceptor of an amide N–H bond located on the opposite side of the C=O bond. This occurs for F NMF*t* and NMA*t* and the water molecule is now perpendicular to the amide plane. This N–H$\cdots$O hydrogen bond is weaker than the previous C=O$\cdots$O or double H–bonds: $D_e \approx 200$ meV and $D_0 \approx 150$ meV. The water and amide dipoles are now aligned so that the total dipole moment is very large, about 6.2–6.6 D, presumably leading to large excess electron binding energies EA_{db}, as compared with all other structures.

Figure 3 also displays approximate values of the intermolecular distances corresponding to the above five types of structures. An other piece of information, which does not appear on this figure, concerns the orientation of the substituted amide methyl groups for water complexes as compared to isolated molecules. For A, B and C conformers, as expected, this orientation does not change because the methyl group is not involved in an interaction with water. On the other hand, we observe that the orientation change upon complexation with water for two A′ conformations over three: for NMF*t* and NMA*t*, the methyl group involved switches from the eclipsed conformation to the staggered one, while the eclipsed conformation is retained for DMF. For B′ conformers, the methyl conformation also remains eclipsed for NMA*t* and remains staggered for NMA*c*. It is not easy to rationalise these results which follow from a subtle competition between intra and inter-molecular interactions.

3.3 Dipole-bound anion excess electron binding energies

From the above calculated neutral complex structures, we now want to evaluate the corresponding expected anion excess electron binding energies $EA_{\rm db}^{\rm th}$, in order to compare those with the experimental values $EA_{\rm db}^{\rm exp}$. Because full quantum calculations of such loosely bound species are very difficult and time consuming [37], we here use a simple electrostatic model which has been previously developed in our group [38]. Briefly, the key ingredients of this model are the following. An electrostatic potential, of cylindrical symmetry, describes the interaction between the polar molecule or complex and the excess electron. It is made of dipole, quadrupole, polarisation and repulsion terms. We thus need as accurate as possible values, for the total dipole moment μ, for the contribution Q of the quadrupole moment tensor on the dipole axis, for the parallel and perpendicular contributions of the polarisability, $\alpha_{\parallel}$ and $\alpha_{\perp}$, and for a repulsion parameter C. The Schrödinger equation is then solved analytically for the angular part and numerically for the remaining one-dimension radial part. We thus obtain the weak binding energy of the excess electron, $EA_{\rm db}^{\rm th}$, together with the characteristics of its diffuse orbital.

The electrostatic parameters of the neutrals are taken as follows. The dipole moment is either the experimental one, when it is available as for the monomers, or, for amide-water complexes, the calculated one corrected from the shift between the calculated and experimental values observed for the monomers. The quadrupole contribution Q is evaluated from the partial atomic charges used in our home-made empirical force field, at the calculated equilibrium geometry of the neutral. The polarisabilities are also evaluated at the calculated neutral geometry, from standard bond polarisabilities [39]. The more critical parameter is the total dipole moment μ together with the repulsion parameter C. This parameter defines two repulsive parallel and perpendicular distances, $r_{\parallel}$ and $r_{\perp}$, below which the Pauli exclusion of the excess electron by the valence electrons becomes predominant: $r_{\parallel} = C\alpha_{\parallel}^{1/3}$ and $r_{\perp} = C\alpha_{\perp}^{1/3}$. With such a definition, C must be close to 1 and it has been empirically fitted to experimental data, as a function of the molecular mean polarisability α, for many dipole-bound anions of isolated molecules [38]. This fit empirically takes into account all quantum non-electrostatic terms in the electron-molecule potential, such as electron correlation [40]. As already observed in previous studies on dipole-bound anions of either isolated molecules or molecular clusters [34,35,38], this procedure works generally well for molecules but is sometimes less accurate for complexes. In the present work, because we deal with molecules or complexes of the same amide family, we use the same parameter for all molecules, $C = 1.13$, and for all complexes, $C = 1.19$. As discussed in the next section, these values appear to give a good agreement between the theoretical and experimental results, for all species of interest.

4 Interpretation and discussion

In this section, for each studied molecular system, we compare the experimental values $EA_{\rm db}^{\rm exp}$ of the excess electron binding energies, deduced from the RET measurements, with the predicted values $EA_{\rm db}^{\rm th}$ obtained from the calculated neutral structures, with the help of the above electrostatic model, for the corresponding dipole-bound anions. In order to validate the procedure, we first examine the four isolated amides and then focus our attention towards their mono-hydrated complexes, in order to determine which complex configurations have been observed. Table 4 sums up the calculated results for all molecules and complexes studied and compares those to experimental values of the observed dipole-bound anions.

4.1 Isolated molecules

For F and DMF molecules, there is only one possible conformer and the theoretical excess electron binding energies are in very good agreement with experimental data, providing that we use the experimental values of the dipole moments. This also true for the *trans* conformer of NMF, even if the *cis* conformer $EA_{\rm db}^{\rm th}$-value could also be compatible with the experimental value, providing that its calculated dipole moment is also decreased by 0.2 D, the difference between calculated and experimental values for the *trans* structure. High-level *ab initio* calculations [21] have already shown that both conformers give birth to dipole-bound anions with similar excess electron binding energies. However, this previous work and the present quantum calculations agree to locate the *cis* conformer of NMF at an energy well above, by at least 40 meV, that of the *trans* conformer, so that it is very likely that the *cis* conformer is only weakly populated in our supersonic beam. This holds even more for NMA since previous [26,27] and present calculations also agree that the energy difference between *cis* and *trans* conformers should be even higher, *i.e.* about 100 meV. As a matter of fact, the experimental $EA_{\rm db}^{\rm exp}$-value is again in very good agreement with the calculated value for NMA*t*, when the dipole moment is taken as the average of the two experimental values, *i.e.* only 0.08 D lower than the present calculated value. On the other hand, $EA_{\rm db}^{\rm exp}$ and $EA_{\rm db}^{\rm th}$ are not compatible for the *cis* conformer, even when the same dipole moment shift is applied. The comparison between calculated and experimental excess electron binding energies is then very good, providing that experimental dipole moments are used instead of calculated values which appear to be always overestimated for all amides: 0.25 D for F, 0.20 D for NMF, 0.08 D for NMA and 0.33 for DMF.

4.2 Mixed amide-water complexes

Among the three equilibrium configurations of the formamide-water neutral complex, only configuration A must be produced in our experimental conditions. In such a supersonic molecular beam, an estimate of the

Table 4. Molecular parameters used for the theoretical estimate of the excess electron binding energies $EA_{\rm db}^{\rm th}$, for the different amide molecules and complexes with water, to be compared with the experimental values $EA_{\rm db}^{\rm exp}$. Species in bold are those who have been observed and assigned from this comparison (see text for discussion).

Molecule or complex	μ (D)	Q (DÅ)	α (Å^3)	$EA_{\rm db}^{\rm th}$ (meV)	$EA_{\rm db}^{\rm exp}$ (meV)
F	3.73	−4	4.2	**15 ± 2**	**16.1**
NMF*t*	3.80	−2	5.9	**16 ± 2**	**15.4**
NMF*c*	4.10	−15	5.9	17 ± 3	
NMA*t*	3.78	−4	7.8	**14.5 ± 3**	**14.8**
NMA*c*	4.14	−9	7.8	19 ± 3	
DMF	3.83	−8	7.8	**13.5 ± 2**	**13.5**
F-water A	2.44	+16	5.7	**2.8 ± 1**	**3.1**
F-water B	3.70	+14	5.7	30 ± 6	
F-water C	6.20	0	5.7	130 ± 15	
NMF*t*-water A′	3.82	+13	7.4	**28 ± 5**	**29 ± 10**
NMF*t*-water B	4.16	+12	7.4	**39 ± 7**	
NMF*t*-water C	6.05	+6	7.4	125 ± 15	
NMF*c*-water A	3.04	+4	7.4	**4.2 ± 1**	**3.5**
NMF*c*-water B	4.25	+6.5	7.4	34 ± 6	
NMA*t*-water B′	4.50	+11	9.3	**45 ± 7**	**33 ± 10**
NMA*t*-water A′	4.33	+5.5	9.3	**30 ± 5**	
NMA*t*-water C	6.56	+ 4	9.3	140 ± 15	
NMA*c*-water A	3.40	0	9.3	7 ± 1	
NMA*c*-water B′	4.78	+2	9.3	42 ± 6	
DMF-water B	4.21	+5	9.3	**28 ± 5**	**24 ± 10**
DMF-water A′	3.97	−4	9.3	**15 ± 3**	

intermolecular temperature is indeed about 150 K (*i.e.* 13 meV) or lower [19]. This means that configurations which are located above the lowest equilibrium structure three times higher in energy, *i.e.* 40 meV, are unlikely to be populated in the beam. Configurations B and C are lying respectively 98 and 132 meV above configuration A. A single peak is indeed observed on the RET curve (Fig. 1a) and the corresponding $EA_{\rm db}^{\rm exp}$-value is in very good agreement with the calculated value providing that the dipole moment is taken as the calculated value lowered by 0.25 D, as for the monomer. B and C configurations would have lead to dipole-bound anions with much higher excess electron binding energies (see Tab. 4), which should have been observed at much lower Rydberg quantum numbers (respectively around $n = 11$ and $n = 6$).

If we now switch to the other simple case of DMF, there are now two possible conformations (A′ and B) with very similar dissociation energies (within 7 meV) and, unfortunately, also similar dipole moments. The RET curve exhibits a single broad peak (Fig. 1d) which probably results from the superposition of the two peaks corresponding to the two types of dipole-bound anions. The experimental excess electron binding energy indeed falls in between the values calculated for the two configurations which calculated dipole moments have been again lowered by 0.33 D, as for the monomer. The difference between the two total dipole moments, 0.24 D, is too low to be resolved by the RET method.

The situation is more complicated for NMF and NMA due to the existence of the two *cis* and *trans* conformers and thus the possibility of three low-lying amide-water configurations. For both NMF and NMA, there are two low-lying *trans* configurations (respectively A′ and B and A′ and B′) with very similar dissociation energies (within 12 or 13 meV) and similar high dipole moments (respective calculated values of 4.02 and 4.36 D and 4.58 and 4.41 D). As for DMF, these pairs of structures are expected to give a single broad peak in the RET curves at low Rydberg quantum numbers, as it is observed. Again, the $EA_{\rm db}^{\rm th}$-values, calculated with dipole moments respectively lowered by 0.20 and 0.08 D as for monomers, fall just below and above the experimental value. As for formamide, the third *trans* configurations C are unlikely to be populated in the beam, because of their much higher energies, and their dipole moments are too high to be compatible with the measured $EA_{\rm db}^{\rm exp}$-values. In addition, for both NMF*c* and NMA*c*, there is also one low-lying configuration (A), with a much higher dissociation energy (about 100 meV higher) and a lower dipole moment (3.2–3.5 D) as compared to the *trans* structures. This configuration, similar to that observed for formamide-water, is expected to give an other RET peak at large Rydberg quantum numbers although this peak is observed for NMF but not for NMA. This is however not so surprising for the following reasons.

As displayed in Figure 4, the *cis* conformer of the isolated molecule is located 43 meV above the *trans* conformer for NMF, and this difference increases to 100 meV for NMA. On the other hand, the *cis* A configuration of the amide-water complex is more bound by about 95 meV with respect to the *trans* A′ and B configurations for NMF,

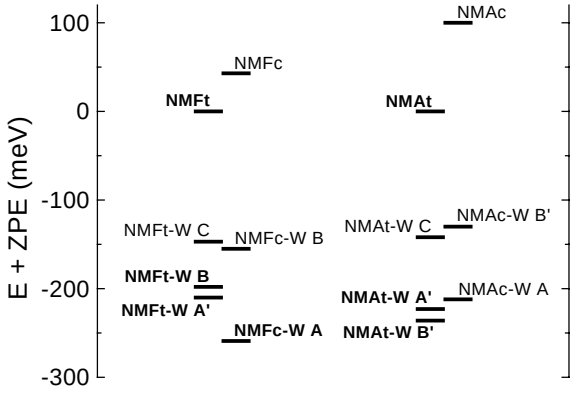

Fig. 4. Relative calculated total energies (corrected from *ZPE*) of the NMF and NMA molecules and of their mono-hydrated complexes. Species in bold are those who have been observed and assigned. See text for discussion.

and by about 80 meV with respect to the *trans* A′ and B′ configurations for NMA. It follows that, for NMF, the *cis* A configuration is more stable than the *trans* A′ and B configurations by about 50 meV, while, for NMA, it is less stable than the *trans* A′ and B′ configurations by about 20 meV. However, if the total complex energies were the only pertinent values for evaluating the complex populations in the beam, the *cis* A configuration would be almost the only configuration populated for NMF, while it would be only slightly less populated than the *trans* A′ and B′ configurations for NMA. On the other hand, one can argue that complex configurations are formed in the beam only from monomer conformations which already exist prior to the beam expansion. Complex populations would then be mainly determined by conformer populations, at the amide reservoir temperature, and thus by the conformer energies of the isolated molecules. In that case, *cis* configurations would be almost not populated for NMF and not at all populated for NMA. It is not possible to get quantitative estimates of the configuration populations from the present data but the observed situation, in which the *cis* A configuration is rather well populated for NMF and not populated for NMA, is clearly intermediate in between the two above descriptions. It seems that, in the case of NMF, at least part of the *trans* (presumably A′) complexes, which are formed in the early stage of the expansion with enough internal energy, can overcome the barrier between the *trans* and *cis* conformations in order to form more stable *cis* A complexes. The resulting complex populations is then the result of a combination of the monomer conformer stabilities, and the barrier height between them, and of the complex stabilities.

5 Conclusion

Rydberg Electron Transfer spectroscopy appears as a suitable method for the determination of structures of hydrated complexes when there are no available chromophores allowing for REMPI or similar spectroscopic techniques. When coupled to accurate structure calculations, as shown in the case of NMF, it can allow for a clear identification of *cis* and *trans* configurations. However, when complexes with similar total dipole moments are populated, the method does not allow for the discrimination between otherwise very different configurations. This is the case of the A′ and B configurations in DMF and NMF*t* or A′ and B′ in NMA*t*. Discrimination would however be possible by coupling infrared (IR) spectroscopy [41] to the present technique, in an IR/RET experiment. The selection of the Rydberg atom, involved in the RET process, would optimise the anion production of the selected complex configurations. Tunable IR excitation of the water or amide O–H or N–H bonds, involved in hydrogen bonding, would lead to predissociation of the neutrals which could then be observed as an ion-dip signal [11].

Among the four investigated molecules, NMA is the most relevant to modelling hydration of proteins. For the parameterization of the peptide backbone, in an all-atom empirical force field, *ab initio* structures interaction energies and dipole moments of NMA-water complexes have been used [42]. Since this study was intended for condensed-phase simulations, this was done for NMA with its condensed-phase geometry. However, structural changes take place between gas-phase and condensed-phase and it might thus be useful to introduce experimentally determined gas-phase structures, such as those presented in the present work, in the parameterization of force-fields which are used in the modelling of gas-phase hydrated peptide ions [43].

References

1. G. Otting, E. Liepinsh, K. Wüthrich, Science **254**, 974 (1991)
2. M.E. Jarrold, Acc. Chem. Res. **32**, 360 (1999)
3. M. Daune, *Molecular Biophysics* (Oxford University Press, Oxford, 1999)
4. K. Nadassy, S.J. Wodak, J. Janin, Biochemistry **38**, 1999 (1999)
5. M.F. Jarrold, Annu. Rev. Phys. Chem. **51**, 179 (2000)
6. M. Mons *et al.*, J. Phys. Chem. **103**, 9958 (1999)
7. J.R. Carney, F.C. Hagemeister, T.S. Zwier, J. Chem. Phys. **108**, 3379 (1998)
8. R.M. Helm *et al.*, J. Phys. Chem. **102**, 3268 (1998)
9. J.E. Braun, T. Mehnert, H.J. Neusser, Int. J. Mass. Spectrom. **203**, 1 (2000)
10. E.G. Robertson *et al.*, J. Phys. Chem. **104**, 11714 (2000)
11. A.V. Fedorov *et al.*, J. Phys. Chem. **105**, 8162 (2001)
12. G.T. Fraser, R.D. Suenram, F.J. Lovas, J. Mol. Struct. **189**, 165 (1988)
13. A. Engdahl, B. Nelander, P.O. Astrand, J. Chem. Phys. **99**, 4894 (1993)
14. E.G. Robertson, Chem. Phys. Lett. **325**, 299 (2000)
15. C.E.H. Dessent, C.G. Bailey, M.A. Johnson, J. Chem. Phys. **102**, 6335 (1995)
16. C. Desfrançois, H. Abdoul-Carime, J.P. Schermann, Int. J. Mod. Phys. **10**, 1339 (1996)
17. G.H. Lee *et al.*, Chem. Phys. Lett. **321**, 333 (2000)

18. S.Y. Han *et al.*, J. Chem. Phys. **109**, 9656 (1998)
19. C. Desfrançois *et al.*, J. Chem. Phys. **102**, 4952 (1995)
20. K. Harth, M.-W. Rüf, H. Hotop, Z. Phys. D **14**, 149 (1989)
21. C. Desfrançois *et al.*, J. Chem. Phys. **110**, 4309 (1999)
22. C. Desfrançois, Phys. Rev. A **51**, 3667 (1995)
23. A.C. Fantoni, W. Caminati, J. Chem. Soc. Faraday Trans. **92**, 343 (1996)
24. D.R. Lide, *CRC Handbook of Chemistry and Physics* (CRC Press, Boca Raton USA, 1995)
25. R.A. Elzaro *et al.*, in *28th Symposium on Molecular Structure and Spectroscopy*, Columbus, OH, USA, 1973, p. 200
26. Y.K. Kang, J. Mol. Struct. **546**, 183 (2001)
27. W.G. Han, S. Suhai, J. Phys. Chem. **100**, 3942 (1996)
28. Y. Bouteiller *et al.*, J. Chem. Phys. **105**, 6420 (1996)
29. H. Abdoul-Carime *et al.*, Z. Phys. D **40**, 55 (1997)
30. A.D. Becke, Phys. Rev. A **38**, 3098 (1988)
31. M.J. Frisch *et al.*, *Gaussian 98*, Revision A.9, Gaussian Inc., Pittsburg, PA, 1998
32. D.E. Woon, T.H. Dunning, J. Chem. Phys. **100**, 2975 (1994)
33. X. Zhou *et al.*, J. Phys. Chem. **100**, 16822 (1996)
34. S. Carles *et al.*, J. Chem. Phys. **112**, 3726 (2000)
35. S. Carles *et al.*, J. Phys. Chem. A **104**, 10662 (2000)
36. F.J. Lovas *et al.*, J. Chem. Phys. **88**, 722 (1988)
37. P. Skurski *et al.*, J. Am. Chem. Soc. **123**, 11073 (2001)
38. H. Abdoul-Carime, C. Desfrançois, Eur. Phys. J. D **2**, 149 (1998)
39. C. Hirschfelder, T. Curtiss, W. Byrd, *Molecular theory of gases and liquids* (John Wiley and Sons Inc., 1975)
40. M. Gutowski, P. Skurski, Rec. Res. Dev. Phys. Chem. **3**, 245 (1999)
41. K. Nauta, R.E. Miller, Science **283**, 1895 (1999)
42. A.D. MacKerrel *et al.*, J. Phys. Chem. **102**, 3586 (1998)
43. J. Woenckhaus, R.R. Hudgins, M.F. Jarrold, J. Am. Chem. Soc. **119**, 9586 (1997)